

NASA TECHNICAL NOTE



NASA TN D-3422

NASA TN D-3422

LOAN COPY: RI  
AFWL (WI  
KIRTLAND AFI



# A SIMPLE ATMOSPHERE REENTRY GUIDANCE SCHEME FOR RETURN FROM THE MANNED MARS MISSION

*by Henry C. Lessing and Robert E. Coate*

*Ames Research Center  
Moffett Field, Calif.*



A SIMPLE ATMOSPHERE REENTRY GUIDANCE SCHEME FOR RETURN  
FROM THE MANNED MARS MISSION

By Henry C. Lessing and Robert E. Coate

Ames Research Center  
Moffett Field, Calif.

NATIONAL AERONAUTICS AND SPACE ADMINISTRATION

---

For sale by the Clearinghouse for Federal Scientific and Technical Information  
Springfield, Virginia 22151 - Price \$2.00

# A SIMPLE ATMOSPHERE REENTRY GUIDANCE SCHEME FOR RETURN

## FROM THE MANNED MARS MISSION

By Henry C. Lessing and Robert E. Coate  
Ames Research Center

### SUMMARY

A study was made to determine the capability of a fixed attitude, roll controlled type of lifting body to accomplish the atmosphere reentry at speeds up to 21 km/sec (maximum estimated speed for return from Mars missions) and to develop a guidance scheme requiring only a limited amount of logic and simple calculations for mechanization.

The effects of variations of vehicle parameters and atmosphere density on the available corridor depth provided by this type of vehicle were investigated and compared with the accuracy attainable by the midcourse guidance. The results indicate that, at the highest velocity expected for return from the Mars mission, sufficient corridor depth to satisfy midcourse guidance accuracy requirements can be achieved with this type vehicle, provided that atmosphere density information is available prior to reentry and provided also that ground-based tracking data are utilized.

It is shown that for this mission and vehicle a simple guidance scheme is capable of satisfying the prime accuracy and acceleration limit constraints on the trajectory.

### INTRODUCTION

A number of studies of the manned Mars mission (see, e.g., ref. 1) have shown that vehicle speeds upon arrival at Earth, depending on launch time and type of trajectory, will range roughly from 15 to 21 km/sec. For these high speeds, the reentry guidance requirements, in terms of vehicle and control parameters which will satisfy mission constraints, may be difficult to meet particularly when there are uncertainties in the atmosphere environment. This problem has been reviewed in reference 2 for various types of vehicles. These requirements are also considered in the present study, specifically for the type of roll control studied so extensively for the lunar mission. The complexity of the guidance which will be necessary for successful reentry at these extreme velocities has not been established. It is possible that by the time of the Mars mission, computer technology will have advanced to the state where the reentry guidance can be based on rapid and repeated integrations of the complete nonlinear equations of motion. In spite of this possibility, it may be desirable to use a simpler primary guidance system or at the very least, to have a simpler system in reserve in case some failure makes the more complex techniques inoperable. It is desirable, therefore, to investigate the

capability of guidance schemes requiring only a limited amount of logic and simple calculations for mechanization. The present paper presents the results of such a study.

#### NOMENCLATURE

|                           |   |
|---------------------------|---|
| A                         | total nongravitational acceleration felt by the pilot, normalized with respect to the acceleration due to gravity at the Earth's surface, $g$ , dimensionless |
| A'                        | $dA/dV$ , $g/(m/sec)$   |
| $C_D$                     | drag coefficient  |
| $h$                       | altitude, m   |
| $K_A, K_{A'}, K_V, K_X$ } | control equation gains  |
| L/D                       | lift-drag ratio   |
| $r$                       | distance from Earth center, $r_0 + h$ , m   |
| $r_0$                     | Earth radius, m   |
| S                         | reference area, $m^2$   |
| V                         | velocity relative to atmosphere, $(V_I - r\omega_0)$ , m/sec  |
| $V_i$                     | initial reentry velocity relative to atmosphere, m/sec  |
| $V_I$                     | velocity relative to Earth centered inertial system, m/sec  |
| $V_0$                     | orbital velocity relative to Earth centered inertial system, m/sec  |
| W                         | vehicle weight at Earth surface, newton   |
| X                         | range, km   |
| $\gamma$                  | flight-path angle, deg  |
| $\phi$                    | roll angle, deg   |
| $\omega_0$                | Earth rotation rate, rad/sec  |

## Subscripts

B bias value  
c command value  
e value at atmosphere exit  
r reference value  
s skip value  
TG to go

### The International System of Units Conversion Factors (See Ref. 3)

| <u>To convert from</u>   | <u>to</u> | <u>multiply by</u>  |
|--------------------------|-----------|---------------------|
| pound force, lb          | newton, N | 4.4482              |
| foot, ft                 | meter, m  | 0.3048              |
| Intl. naut. mile, n. mi. | meter, m  | $1.852 \times 10^3$ |

## REENTRY CORRIDOR

The vehicle considered in this study was of the fixed trim, lifting body type, which is controlled by rolling the vehicle to properly orient the resultant lift vector. The pertinent characteristics of such a vehicle are the lift-drag ratio,  $L/D$ , the ballistic parameter,  $W/C_D S$ , and the roll dynamics.

Point mass equations of motion in the presence of a spherical rotating Earth were used in this study (ref. 4); however, the trajectory of the vehicle was restricted to the equatorial plane, with the vehicle flying in the direction of Earth's rotation. It should be noted that a fixed trim, roll controlled vehicle cannot be constrained to two-dimensional flight, but will move in a lateral direction as the resultant lift vector is oriented to produce the appropriate vertical value for longitudinal range control. Zero lateral range dispersion at the destination must be achieved by alternately orienting the resultant lift vector to the left and right of vertical. The lateral motions resulting from this type of control were not considered in the present study.

The standard atmosphere was assumed to be the 1959 ARDC model (ref. 5), and the assumed variation about this standard (shown in fig. 1) was taken from reference 6. This magnitude of variation appears to be extreme on the basis of later information (ref. 7), but this is a desirable condition for the simulation of problems associated with uncertain density.

The variation of reentry corridor depth (defined in ref. 8) with variation of vehicle lift-drag ratio is shown in figure 2 for a velocity of 21,336 m/sec (70,000 ft/sec). These results show that increasing L/D provides increasingly smaller increments in corridor depth. Various lifting body types of vehicles have been proposed but those with values of lift-drag ratio significantly greater than unity are probably unrealistic. The results in figure 2 thus indicate that if the atmosphere characteristics are known prior to reentry, a corridor depth of the order of 17 km is available. If, however, an uncertainty exists as to the characteristics of the atmosphere between the extremes assumed previously, then the available corridor shrinks as shown in figure 2. The reason for this can be seen in figure 3, where the reentry corridor is presented in terms of initial flight-path angle at an altitude of 122 km (400,000 ft). The angle increment between the capture and 10 g boundaries defines the corridor "depth" in this figure. The relationship between this angle increment and corridor depth in nautical miles is given in reference 8. It can be seen in figure 3 that at a velocity of 21 km/sec, the angle increment between the capture boundary and the 10 g boundary is essentially the same for the increased, standard, and decreased density atmospheres. Thus, if the type of atmosphere is known prior to reentry, the spacecraft may be controlled to a desired flight-path angle within the boundaries corresponding to that atmosphere. The available or usable corridor depth is then essentially independent of the type of atmosphere, and the upper curve of figure 2 results. If, however, an uncertainty exists as to the type of atmosphere, then to ensure a safe reentry, the flight-path angle must be restricted to a value common to the possible atmosphere extremes. Values common to the extremes assumed in this study, shown in figure 3 by the superimposed crosshatching, correspond at 21 km/sec to the lower curve of figure 2.

It is of interest to compare these results with the accuracy attainable by the midcourse guidance. Reference 9 shows that, for a completely on-board operation, the spacecraft could be guided to a corridor approximately 10 km deep. This is a  $1\sigma$  value, however, and therefore the probability of success in meeting even the best corridor capability of figure 2 appears to be unacceptable. However, an unpublished extension of the study of reference 9 includes the use of ground based tracking data and indicates an ability to guide to approximately a 4.5 km corridor ( $1\sigma$ ). Using a safety factor of 3 as an acceptable probability of success gives a required corridor of approximately 13.5 km, an accuracy adequate for the corridor shown in figure 2 for a known atmosphere. It is still insufficient if the atmosphere characteristics are unknown and the possible density variations are of the magnitude assumed in this study. As mentioned previously, these density variations are thought to be extreme; but considering how little corridor loss is possible before midcourse accuracy restrictions are violated, it appears that for an  $L/D = 1$  vehicle, atmosphere density information will almost be a necessity. This problem can be alleviated through the use of a vehicle with greater corridor capability, such as a variable pitch attitude type (ref. 10).

The results in figures 2 and 3 are for a vehicle with a ballistic parameter equal to  $9576 \text{ N/m}^2$  (200 lb/sq ft). As shown in reference 8, the effects of ballistic parameter variations on corridor depth are relatively minor. In subsequent portions of the report the effects of this parameter on various aspects of the guidance problem are discussed.

The effect of roll dynamics on available corridor depth was investigated in reference 2. It was shown that although timing was critical, the use of roll dynamics comparable to those for the Apollo vehicle caused very little corridor loss. This point is discussed subsequently in the development of the guidance. The assumed roll dynamics were

|                           |                             |
|---------------------------|-----------------------------|
| Maximum roll acceleration | $\pm 10^\circ/\text{sec}^2$ |
| Maximum roll rate         | $\pm 20^\circ/\text{sec}$   |
| Roll-rate deadband        | $\pm 2^\circ/\text{sec}$    |
| Roll-angle deadband       | $\pm 4^\circ$               |

#### Guidance Phases

The three phases of the reentry guidance problem considered in this paper (fig. 4) are capture and acceleration control phase, which extends from initial contact with the atmosphere until approximately horizontal flight is achieved; skipout control phase, which occurs essentially at circular orbital speed; and terminal control phase, which extends from circular speed until the destination is reached. Terminal here refers not to the type of guidance, but to the fact that the vehicle is at subcircular speed and near its destination.

The state variables used for guidance information are range, velocity, acceleration, and rate of change of acceleration with velocity. The first three variables are natural guidance quantities, acceleration being a basic measurement obtained from the inertial equipment on board the spacecraft; velocity, a fundamental measure of the spacecraft energy; and range, the quantity to be controlled. Rate of change of acceleration with velocity is used as the fourth necessary variable and is readily accessible from the values of acceleration and velocity already available.

In terms of these variables, a general control equation can be written as

$$(L/D)_c = (L/D)_r + K_A(A - A_r) + K_A'(A' - A_r') + K_V(V - V_r) + K_X(X_{TG} - X_{TG_r}) \quad (1)$$

where  $-(L/D) \leq (L/D)_c \leq (L/D)$  and  $(L/D)_c$  is the command value of the vertical component of the total fixed lift-drag ratio,  $(L/D)$ , of the vehicle. The appropriate roll-angle command is then

$$\cos \varphi_c = \frac{(L/D)_c}{L/D} \quad (2)$$

As written, the gains and reference values of the state variables in equation (1) are generally expressed as functions of time. In the following applications of equation (1) to the various guidance phases, time will not be used as the independent variable, and only the state variables relevant to the primary requirements and constraints of a particular phase will be used. It will also be seen subsequently that explicit implementation of the last two terms in equation (1) is unnecessary, but that these state variables are included in other terms.

## Capture and Acceleration Control

The first phase considered is capture and acceleration control. Figure 5 shows the initial variation of acceleration with velocity for the vehicle reentering the Earth's atmosphere at 21,336 m/sec (70,000 ft/sec). In this and the subsequent reentry examples, only this speed is shown because it is the most critical reentry condition, and guidance techniques developed for this speed are applicable to slower reentries. The two acceleration traces shown are for reentries at angles corresponding to the extremes of the corridor, the capture boundary, and the 10 g boundary. The curve labeled  $\gamma = 0^\circ$  boundary corresponds to those combinations of acceleration and velocity for which full negative lift is necessary to maintain level flight and to remain in the atmosphere. Thus the acceleration level for any trajectory must be controlled to a value between this boundary and the maximum allowable acceleration of 10 g until a velocity suitable for initiating the skipout control phase has been reached.

In order to provide the prediction information necessary to initially control the vehicle to the required acceleration level, the two trajectories of figure 5 may be utilized as shown in figure 6. This figure presents the variation of rate of change of acceleration with velocity,  $A'$ , with acceleration,  $A$ , for the two reentries prior to the condition  $A' = 0$ . A reference trajectory may be defined essentially as the median curve. This simple specification of the reference trajectory in the  $A, A'$  plane reflects the fact that during the first phase the only concern is that of ensuring aerodynamic capture and complying with the maximum acceleration constraint. Control about this reference may then be simply specified as

$$(L/D)_c = K_A'(A' - A_r') \quad (3)$$

If the  $A_r'$  versus  $A$  variation for the reference trajectory is obtained for the range of expected reentry velocities  $V_i$ , then it is possible to express the reference trajectory as  $A_r' = f(A, V_i)$ . Alternatively, it is possible to obtain plots similar to figure 6 for a fixed velocity  $V$ . The boundary shapes are almost the same as shown in figure 6; the primary difference is that the capture boundary reaches  $A' = 0$  at a higher acceleration. Again, obtaining the variation for a range of velocities enables the reference trajectory to be expressed as  $A_r' = f(A, V)$ . In the present study the simplifying assumption was made that the reference trajectory shape of figure 6 represented that for a fixed velocity  $V$ ; the velocity effects were found to be adequately accounted for by simply specifying  $A_r'$  as

$$A_r' = f_1(A)f_2(V) \quad (4)$$

Since  $A' = 0$  when the vehicle is outside the atmosphere, equation (3) cannot be used to determine vehicle attitude until the reentry has progressed to some extent. Prior to reentry, on-board inertial measurements will indicate whether the reentry is occurring near the overshoot or the 10 g boundary, and the necessity of an initial roll angle of  $180^\circ$  or  $0^\circ$  can thus be determined. If the reentry is at a more intermediate location in the corridor the initial roll angle value is immaterial. This guidance phase is therefore initiated by maintaining the appropriate roll angle until the acceleration has become

sufficient for accurate implementation of equation (3). The vehicle is then controlled by equations (3) and (4) and the reference trajectory of figure 6 until  $A'$  reaches zero, which corresponds approximately to horizontal flight. At this point the capture and acceleration control phase is completed, but the vehicle must continue to be controlled to an appropriate acceleration level until skipout control is initiated. In the present study the vehicle was simply controlled to a constant acceleration level of 10 g. This point will be discussed subsequently.

The effect of variations of vehicle characteristics on the reentry boundaries is shown in figure 7. The results show that the boundaries are essentially independent of variations in ballistic parameter (fig. 7(a)), but somewhat sensitive to variations in lift-drag ratio (fig. 7(b)). It should be noted that the variations in  $L/D$  due to such varying factors as Mach number, Reynolds number, or heat-shield ablation will be known in advance and the vehicle designed accordingly to provide a suitable "corridor" in the  $A, A'$  plane. The remaining uncertainties should have relatively small effects on the reentry boundaries.

The uncertainties regarding the atmosphere density profile cannot be assumed to be small, and it is important that the reentry boundaries be insensitive to such variations. Figure 8 shows that this is the case; the boundaries are almost invariant with changes in density profile which, as mentioned previously, are probably extreme.

Although roll dynamics considerations do not enter the determination of the reentry boundaries, the ability of the vehicle to be controlled near these boundaries is directly affected by such considerations. Reentry at the capture boundary involves changing from full negative lift to the somewhat less negative value necessary for level flight, which is a rather easy control task. However, the maximum acceleration reentry must be made at full positive lift to avoid exceeding 10 g, after which large negative lift must be achieved to prevent subsequent uncontrollable exit from the atmosphere. The rapidity with which the lift vector can be varied depends directly on the roll dynamics of the vehicle. In general, for reasonable roll dynamics, considerable time is required to execute the required lift reversal; consequently, this maneuver must precede to some extent the point of maximum acceleration. This action, however, will cause the vehicle to exceed the maximum acceleration constraint unless the entry angle is made shallower. Thus, a tradeoff occurs in exchanging corridor depth for slower roll dynamics, but as shown in reference 2, the corridor loss due to using roll dynamics comparable to that of the Apollo spacecraft is negligible if perfect prediction information is available. The less-than-perfect prediction of the simple reference trajectory guidance just discussed causes some additional loss of corridor depth, but as will be seen subsequently, the loss is relatively small.

### Skipout Control

For long ranges (more than 7500 km), it is generally necessary for a reentry vehicle to execute a controlled skipout of the atmosphere. For shorter ranges (less than 7500 km), the skip phase is unnecessary.

The guidance designed to control the trajectory during the skipout phase is basically that developed in reference 11. The range that a vehicle will traverse in a ballistic trajectory outside the atmosphere is a function only of the velocity and the angle between the velocity vector and the local horizontal at the time the vehicle leaves the atmosphere. For a given atmosphere and given vehicle, these variables can be related to two of the variables used in the present study, namely, velocity and rate of change of acceleration with velocity. Since  $A' = A = 0$  when the vehicle is outside the sensible atmosphere, skip range must be related to  $A'$  while the vehicle is still in the atmosphere to the extent that measurable increments of acceleration and velocity are still occurring.

In this study, skip range is defined as the range traversed by the vehicle from the condition  $A = 0.2 g$  during atmosphere exit to zero altitude after the second reentry. Data were obtained from computer solutions of the equations of motion by initiating trajectories at various combinations of  $A'$  and  $V$  at  $A = 0.2 g$ . The vertical component of lift was set to zero during the atmospheric portion of these trajectories. These data are presented in figure 9 in terms of  $A_e'$  ( $A'$  at  $A = 0.2 g$ ) and  $V_e$  (velocity at  $A = 0$  determined from  $A_e'$  and  $V$  at  $A = 0.2 g$ ). The shaded area for each exit velocity in figure 9 shows the effect upon skip range caused by the assumed atmosphere density variations.

To simplify the use of these data as the basis for skipout control, they are represented in the following quadratic form

$$X_s = a + bA_e' + cA_e'^2 \quad (5)$$

and the coefficients  $a$ ,  $b$ , and  $c$  are stored as functions of  $V_e$ . The ability of an equation of the form of equation (5) to fit the data is shown by the solid lines in figure 9. It can be seen that for values of  $A_e'$  greater than approximately  $0.0025 g/(m/sec)$  the fit is relatively good; the greatest dispersion from the computed value due to density variations is of the order of 463 km.

Equation (5) is used to control skipout by means of an iterative computation loop as follows: the actual value of  $A'$  experienced by the vehicle is entered in equation (5) and  $V_e$  is varied until the skip-range value predicted by equation (5) is equal to the desired skip range (where the desired skip range is equal to the range to go minus some small range increment sufficient to cause the termination at the end of the skip to be approximately in the center of the terminal range capability). A reference value of  $A'$  is then computed as that which will take the vehicle from its present values of acceleration and velocity to zero acceleration at the computed  $V_e$ . That is,

$$A_r' = \frac{A}{V - V_e} \quad (6)$$

This value of  $A_r'$  is used in the control equation, which is again given by equation (3). As the vehicle maneuvers in response to the commands of equation (3), a new value of  $V_e$  is continuously computed from equation (5)

according to the varying value of  $A'$ . This process continues until  $A'$  converges to the value given by equation (6). The resulting  $A'$  and  $V_e$  represent the proper combination of these variables that will cause the vehicle to exit at the conditions necessary to achieve the desired skip range. As the vehicle approaches the atmosphere exit condition, however, acceleration approaches zero,  $V$  approaches  $V_e$ , and equation (6) approaches indeterminacy, with resulting inaccurate control. Since the vehicle is essentially out of the atmosphere at this point, erroneous maneuvering due to this indeterminacy has generally negligible effect upon skip range.

The skipout control phase is terminated at circular velocity. The velocity at which this phase is initiated is essentially governed by the accuracy of the skip-range computation and the vehicle roll dynamics. As mentioned previously, figure 9 shows that reasonably accurate skip-range computations are guaranteed only if  $A_e'$  is greater than approximately 0.0025 g/(m/sec). This places an effective lower bound on  $A_e'$ . The upper bound, approximately equal to the maximum value shown in figure 9, is primarily a function of the vehicle roll dynamics, which restrict the rapidity with which the vehicle can be maneuvered. This guidance phase must then be initiated so that the value of  $A_e'$  necessary to achieve the desired skip range is intermediate to these bounds. It is obvious from the wide range of permissible values that the initiation of this phase is not a critical matter.

Since the data and the resulting computations described for this phase are valid only for a specific vehicle and a specific atmosphere, the question of accuracy in the presence of changes of these variables must again be answered. It has already been mentioned that the greatest dispersion in skip range from the computed value due to atmosphere density variations is approximately 463 km. The results obtained for trajectories of 20,372 km (11,000 n. mi.) show no measurable effect of 25-percent variations of ballistic coefficient, but a dispersion of approximately 120 km (65 n. mi.) from 25-percent variations of  $L/D$ . Thus, due to these effects, skip-range error can be approximately 583 km (315 n. mi.). The greatest part of this error, that due to the atmosphere variations, is probably overestimated. However, this magnitude of error generally is easily compensated for by the terminal control, as will be seen in the next section.

#### Terminal Control

The third phase, terminal control, is initiated as the speed becomes sub-circular. Figure 10 illustrates a guidance scheme with the accuracy desired for this phase which is extremely simple. The scheme is based upon flight at constant drag. This is one of the many approximate closed form solutions of the equations of motion that have been proposed as a basis for guidance for many years (ref. 12) and has been used recently (ref. 13) as the basis for a manual reentry guidance scheme. Figure 10 presents range to go to the destination versus the square of velocity, coordinates in which constant drag trajectories appear as straight lines. For the type of vehicle we are considering, constant drag implies constant total nongravitational acceleration, which is shown in the figure. The equation of these trajectories is given by

$$X_{TG} = \frac{V^2 \sqrt{1 + (L/D)^2}}{2(9807)A} \quad (7)$$

which contains the assumption that the flight-path angle  $\gamma$  is sufficiently small to equate  $\cos \gamma = 1$ . This assumption is badly violated because these trajectories terminate in low velocity flight with  $\gamma = -90^\circ$ . However, over most of the trajectory the assumption is valid, and it can be shown that the maximum error in equation (7) caused by the assumption is of the order of 11 km (6 n. mi.). Closed-loop control based on equation (7) eliminates even this small error. The control equation used is, from equation (1),

$$(L/D)_c = (L/D)_r + K_A(A - A_r) + K_{A'} A' \quad (8)$$

where  $A_r$  is obtained from equation (7), and the acceleration rate gain is adjusted for desirable trajectory damping. Since  $\gamma$  is small over most of the trajectory,  $(L/D)_r$  can be approximated by the level flight value as

$$(L/D)_r = \frac{(V_0^2 - V_I^2) \sqrt{1 + (L/D)^2}}{(9.807)rA_r} \quad (9)$$

Including this term in equation (8) is not actually a necessity; the guidance works quite well without it, but its use smoothes the control action by permitting a smaller gain on the acceleration error term. Equations (7) through (9) define a guidance scheme that is extremely accurate because of the basic accuracy of the solution (eq. (7)) used, and also because of the scheme's relative insensitivity to the vehicle characteristics and independence of atmosphere variations. In both equations (7) and (9) the lift-drag ratio of the vehicle enters only through the radical. The ballistic parameter  $W/C_D S$  and the atmosphere density affect only the altitude at which the vehicle must fly in order to generate the desired acceleration, and thus have no effect on the range accuracy.

The vehicle characteristics are important in the restrictions they impose on this scheme. For instance, the vehicle under consideration with an  $L/D$  equal to unity is unable to reach the destination by following the trajectories which intersect the minimum velocity boundary shown in figure 10. This boundary is defined by the velocity at which equation (9) becomes equal to  $L/D$ . The asymptotic value of acceleration on this boundary can be obtained approximately from equation (9) as

$$A_{\min} = \frac{(V_0^2 - r_o^2 \omega_o^2) \sqrt{1 + (L/D)^2}}{(9.807)r_o(L/D)} \quad (10)$$

which represents the minimum acceleration trajectory the vehicle is capable of following. As shown in figure 10 by the dashed constant acceleration trajectory, the limiting value for the vehicle under consideration is about 1.4 g. Thus, whenever a trajectory is initiated in the portion of the figure to the right of the minimum velocity boundary and above the 1.4 g line, the vehicle

must be commanded to pull up until the trace crosses the 1.4 g line, after which it can control to the constant acceleration trajectory necessary to reach the destination. This is accomplished by introducing a bias acceleration  $A_B$  so that, in equation (8),

$$A_r = A_c + A_B \quad (11)$$

where  $A_c$  is obtained from equation (7) as

$$A_c = \frac{v^2 \sqrt{1 + (L/D)^2}}{2(9807)X_{TG}} \quad (12)$$

and

$$\left. \begin{aligned} A_B &= K(A_c - A_{min}) && \text{for } A_c < A_{min} \\ &= 0 && \text{for } A_c > A_{min} \end{aligned} \right\} \quad (13)$$

where  $A_{min}$  is given by equation (10).

Application of this scheme is illustrated by the two trajectories shown in figure 10. While flying the upper trajectory the vehicle is commanded to pull up until the trace achieves the 1.4 g line. The fact that it does so only at the end indicates that it is the maximum range trajectory for the given initial conditions. These conditions correspond to final reentry from a steep, long range skip. A reentry with the same initial conditions but much closer to the destination is shown by the lower trace. This is close to the minimum range trajectory for these initial conditions. The 4445 km initial range increment between these two trajectories shows that this scheme is capable of easily handling the range dispersions caused by the skipout control inaccuracies described in the previous section.

#### Guidance Capability

Integrating the logic of the three guidance phases produces an over-all guidance scheme capable of utilizing almost full vehicle capability. This can be seen from the comparison in figure 11 where the initial flight-path angle limits and range limits are shown for a reentry velocity of 21,336 m/sec (70,000 ft/sec). The flight-path angle limits refer to the two boundaries considered previously corresponding to the standard atmosphere. The minimum range boundary corresponds to the range traversed by a trajectory which maintains a 10 g acceleration, and the maximum range of 20,372 km (11,000 n. mi.) is simply the limit of the investigation. The shaded portion of the corridor corresponds to the capability of the guidance scheme, and it can be seen that the scheme imposes little restriction on the vehicle. Inability to guide from the 10 g boundary is the penalty, mentioned previously, due to the imperfect prediction information available during the capture and acceleration control phase. These results in figure 11 are subject to the assumption made throughout the study that no lateral maneuvering occurs, and that no error exists in the measurement

of the state variables used for guidance information. The magnitude of the effects due to removing these assumptions is a subject for further investigation.

Figure 12 shows two typical trajectories for entries at the extremes of the corridor of figure 11. The lower portion of the figure presents the entire altitude-range histories of both trajectories. In the upper portion of the figure the acceleration-velocity traces are shown from initial reentry to skipout only.

As mentioned previously, and as shown in figure 12, subsequent to the capture and acceleration control phase the vehicle is controlled to a constant 10 g trajectory until the skipout control phase is initiated. Data on human time tolerance to acceleration from reference 14 indicate that a constant 10 g acceleration is tolerable to a human pilot for approximately 1 minute, whereas reentries such as shown in figure 12 result in an exposure to a 10 g acceleration for approximately 3 minutes. This clearly emphasizes that, in the absence of means to increase human tolerance to acceleration, the trajectory shapes shown in figure 12 must be varied to lower acceleration levels. Information on human tolerance to time-varying acceleration levels is not available in the literature, however. An "acceleration-tolerance-rate" function was defined in reference 15 as a means of utilizing constant-acceleration data in time-varying situations. While the definition of this function seems plausible, its true applicability is unknown, and human acceleration tolerance should be investigated further for variable acceleration. When this information becomes available, control to a simple reference trajectory designed to satisfy the resulting constraints should be possible with no increase in controller complexity. The effect of these considerations on the guidance capability shown in figure 11 should be fairly small; an increase in the value of minimum range must occur as the acceleration level is reduced, but guidance capability in the remainder of the corridor should be unaffected.

#### RÉSUMÉ

A study has been made of a reentry vehicle and guidance scheme as applied to the manned Mars mission. The analysis was primarily for 21 km/sec, the highest expected return velocity.

A fixed attitude, roll controlled type of lifting vehicle with L/D of 1 provides sufficient reentry corridor depth to satisfy midcourse guidance accuracy requirements, provided accurate atmosphere density information is available prior to reentry, and provided ground based tracking data are utilized. Consistent with these assumptions and ignoring lateral maneuvers, a guidance system using limited logic requirements and simple calculations for mechanization can satisfy the accuracy and acceleration limit constraints on the trajectory.

Extended periods of acceleration occur during reentries at the higher return velocities associated with the manned Mars mission; this requires further investigations of human tolerance to time varying acceleration.

Ames Research Center  
National Aeronautics and Space Administration  
Moffett Field, Calif., Feb. 16, 1966

#### REFERENCES

1. Sohn, R. L., ed.: Manned Mars Landing and Return Mission. Vol. 1: Summary. Rep. 8572-6011-RU-000, Contract NAS 2-1409, TRW Space Tech. Labs. Inc., March 1964.
2. Wingrove, Rodney C.: Trajectory Control Problems in the Planetary Entry of Manned Vehicles. AIAA Entry Technology Conference, Williamsburg and Hampton, Virginia, Oct. 12-14, 1964, pp. 22-33 (AIAA Pub. CP-9).
3. Mechtly, E. A.: The International System of Units. Physical Constants and Conversion Factors. NASA SP-7012, 1964.
4. Fogarty, L. E.; and Howe, R. M.: Flight Simulation of Orbital and Reentry Vehicles. ASD Tech. Rep. 61-171, Michigan Univ., Oct. 1961.
5. Minzner, Raymond A.; Champion, K. S. W.; and Pond, H. L.: The ARDC Model Atmosphere, 1959. AFCRC-TR-59-267, 1959.
6. Smith, Orvel E.; and Chenoweth, Halsey B.: Range of Density Variability From Surface to 120 KM Altitude. NASA TN D-612, 1961.
7. Anon.: U. S. Standard Atmosphere. U. S. Govt. Printing Office, Washington, D. C., December 1962. (Sponsored by NASA, U.S.A.F., U. S. Weather Bur.)
8. Chapman, Dean R.: An Analysis of the Corridor and Guidance Requirements for Supercircular Entry Into Planetary Atmospheres. NASA TR R-55, 1960.
9. White, John S.; Callas, George P.; and Cicolani, Luigi S.: Application of Statistical Filter Theory to the Interplanetary Navigation and Guidance Problem. NASA TN D-2697, 1965.
10. Becker, J. V.; Baradell, D. L.; and Pritchard, E. B.: Aerodynamics of Trajectory Control for Re-entry at Escape Speed. Astronautica Acta, vol. VII, Fasc. 5-6, 1961, pp. 334-358.
11. Lessing, Henry C.; and Coate, Robert E.: Guidance of a Low L/D Vehicle Entering the Earth's Atmosphere at Speeds up to 50,000 Feet per Second. NASA TN D-2818, 1965.

12. Eggleston, John M.; and Young, John W.: Trajectory Control for Vehicles Entering the Earth's Atmosphere at Small Flight-Path Angles. NASA TR R-89, 1961.
13. Tannas, Lawrence E., Jr.: A Manual Guidance Scheme for Supercircular Entries. Proc. Third Manned Space Flight Meeting, AIAA Pub. CP-10, 1964. Also, AIAA J. Spacecraft and Rockets, vol. 3, no. 2, Feb. 1966, pp. 175-181.
14. Smedal, Captain Harald A., USN(MC); Creer, Brent Y.; and Wingrove, Rodney C.: Physiological Effects of Acceleration Observed During a Centrifuge Study of Pilot Performance. NASA TN D-345, 1960.
15. Bryson, Arthur E.; Denham, Walter F.; Carroll, Frank J.; and Mikami, Kinya: Determination of Lift or Drag Programs to Minimize Re-entry Heating. J. Aerospace Sci., vol. 29, no. 4, April 1962, pp. 420-430.

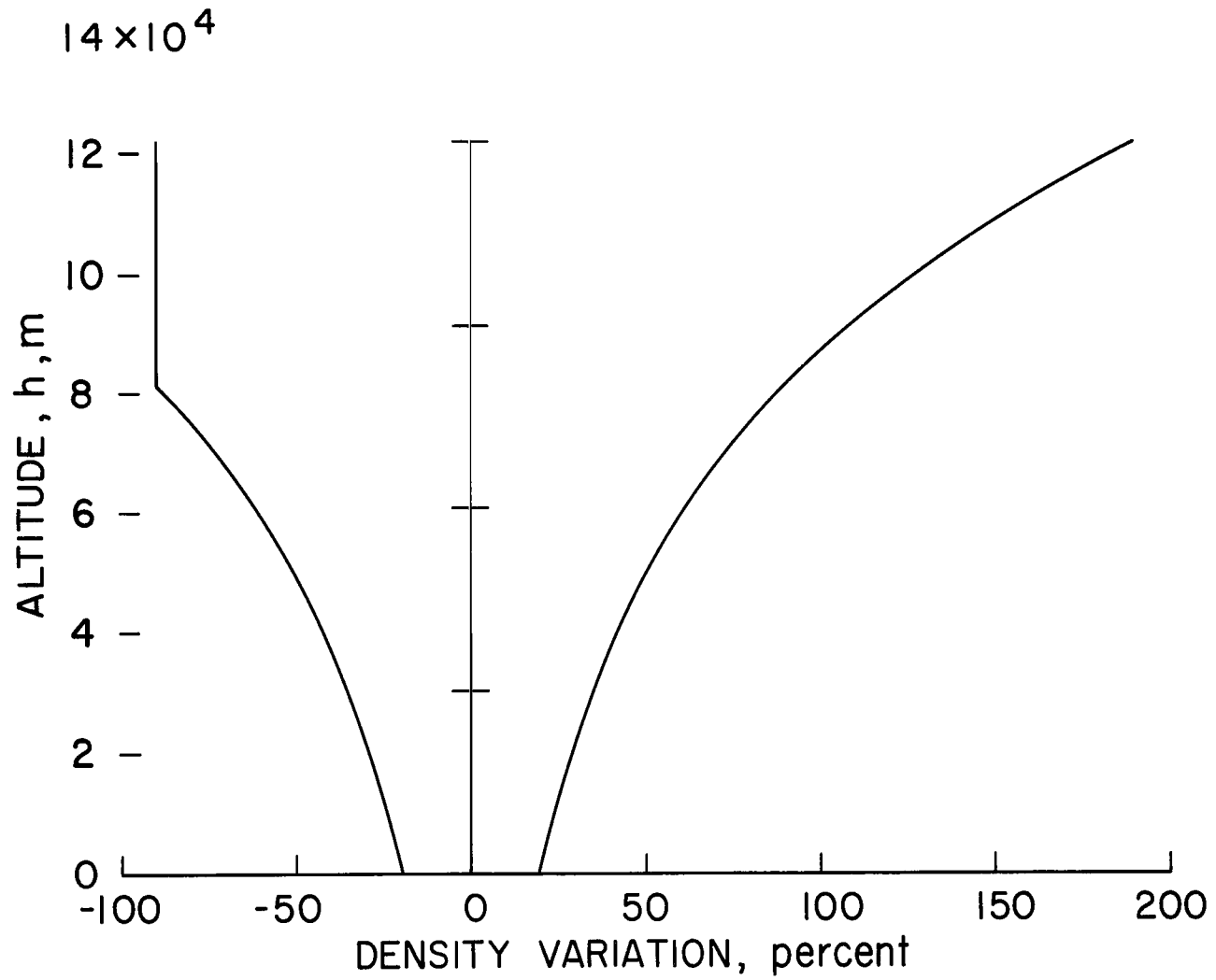


Figure 1.- Density variation about 1959 ARDC model atmosphere.

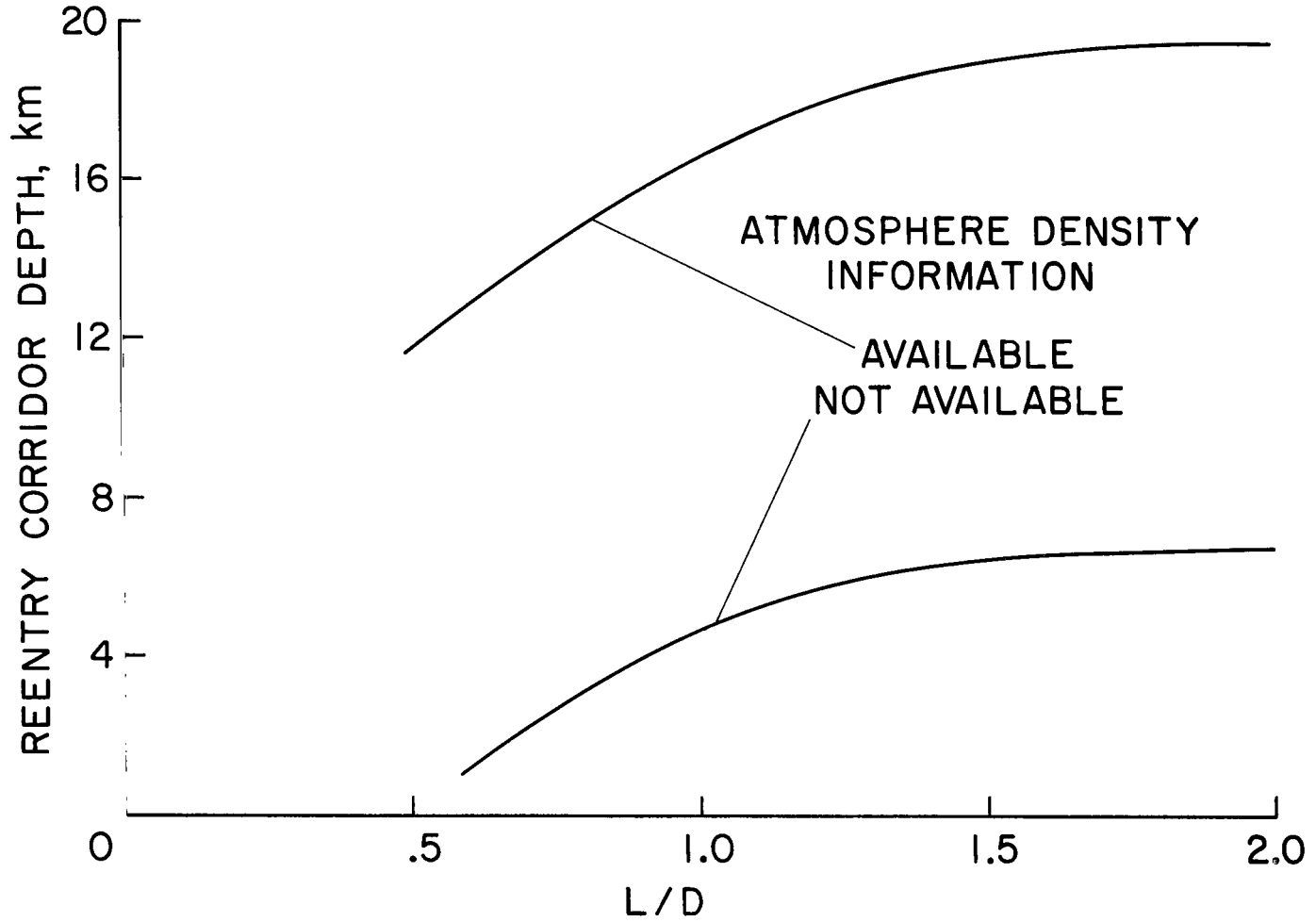


Figure 2.- Effect of atmosphere density information on usable corridor depth;  $V = 21,336$  m/sec,  
 $W/C_D S = 9,576$  N/m<sup>2</sup>.

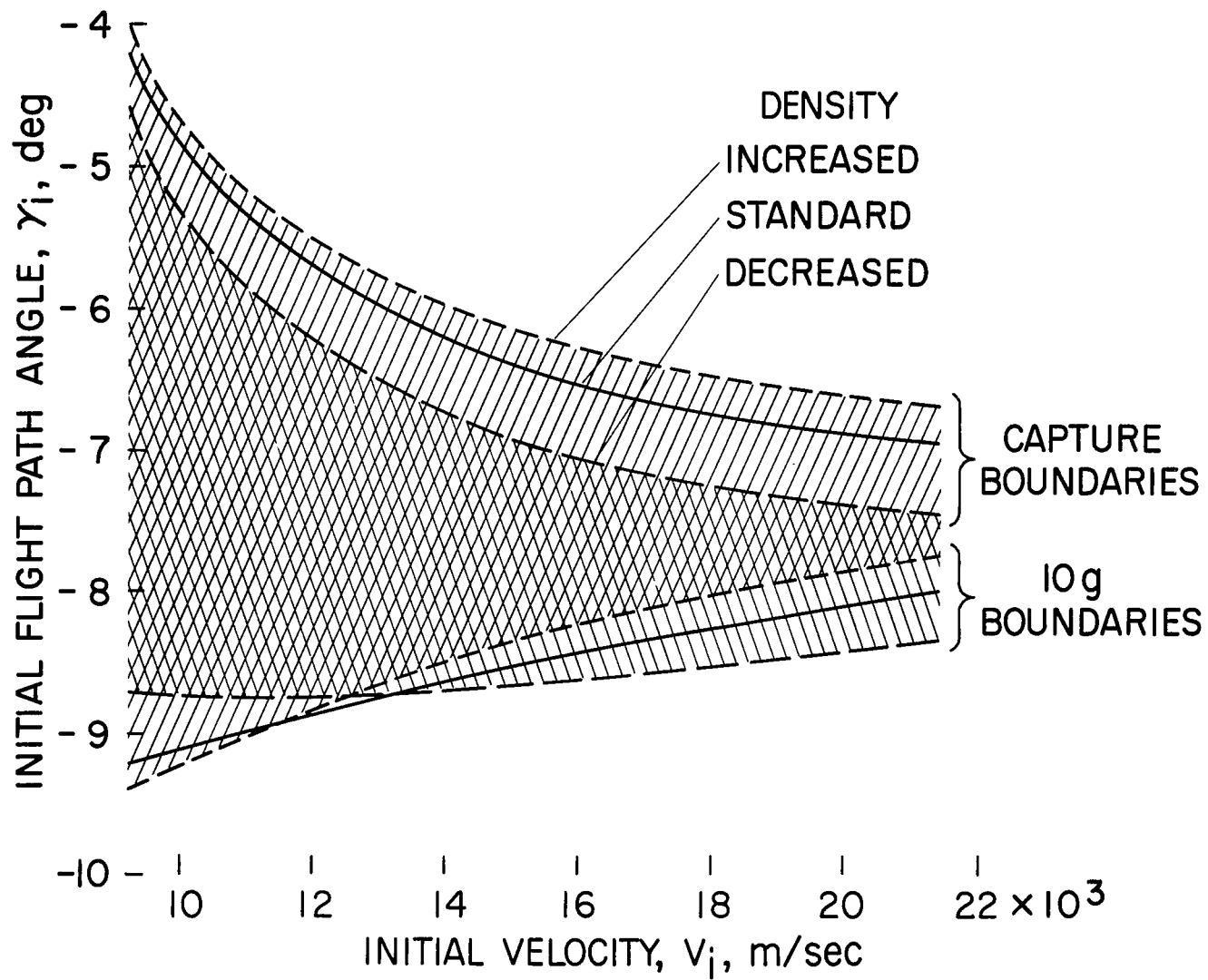


Figure 3.- Reentry corridor for  $L/D = 1.0$ ;  $W/C_D S = 9576 \text{ N/m}^2$ .

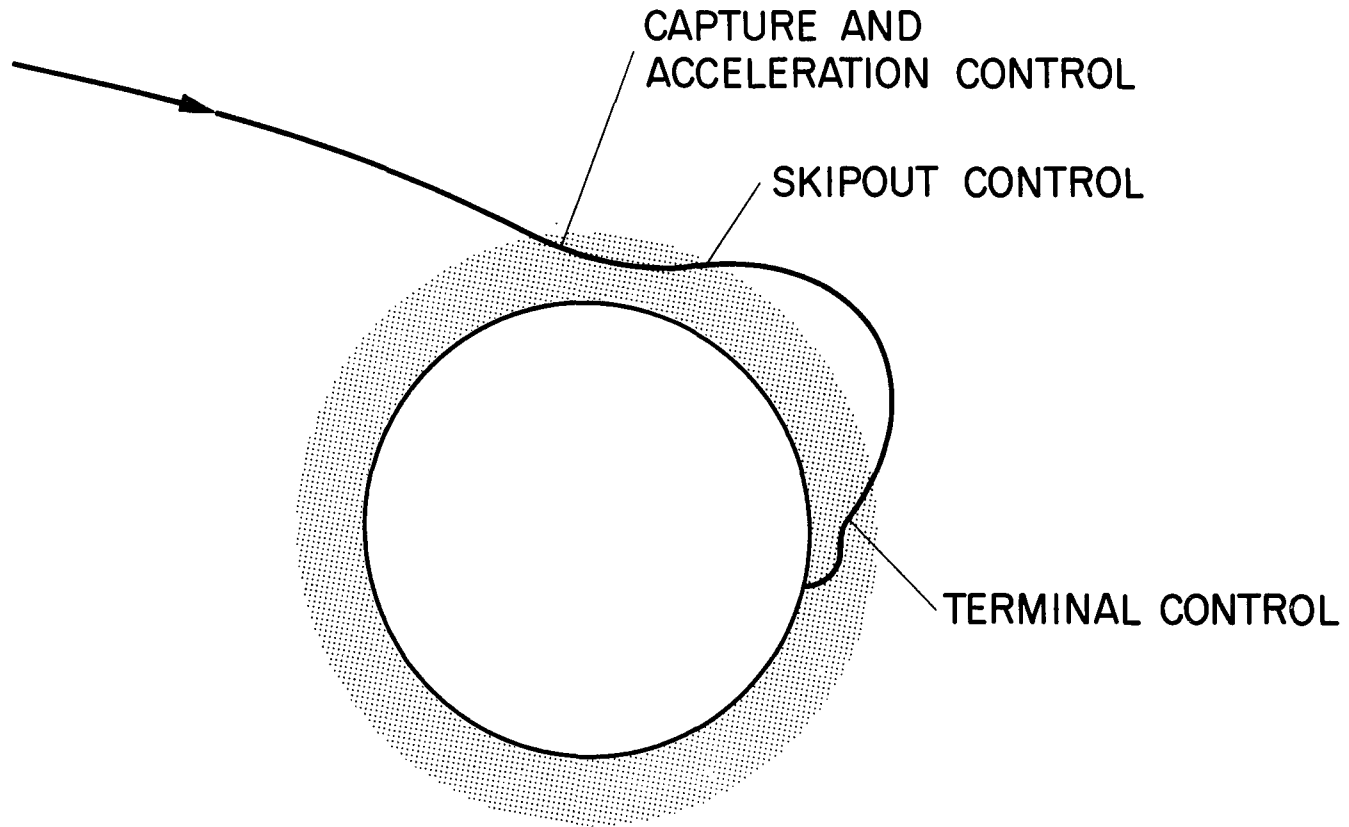


Figure 4.- Reentry guidance phases.

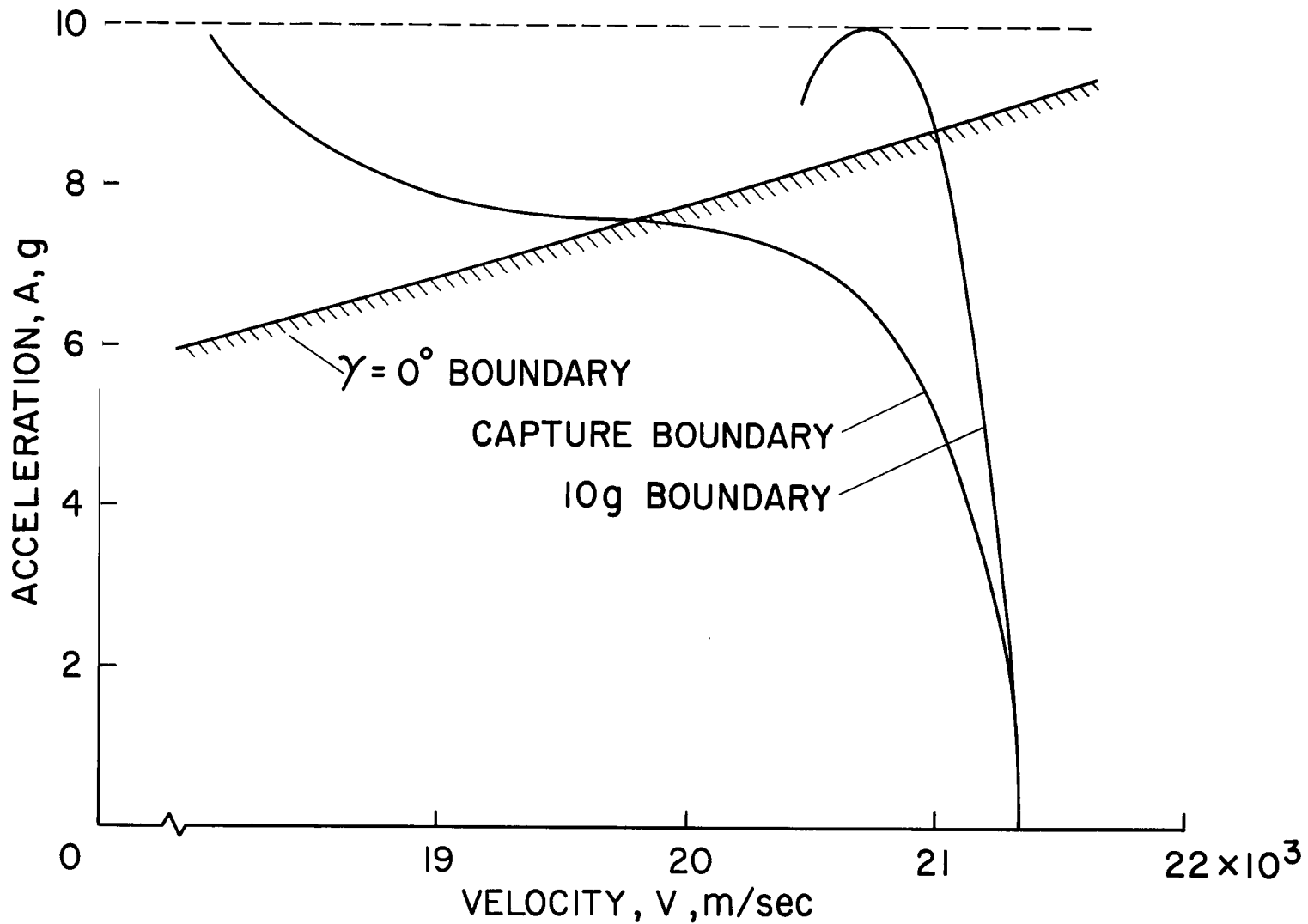


Figure 5.- Acceleration-velocity histories;  $L/D = 1.0$ ,  $W/C_D S = 9576 \text{ N/m}^2$ .

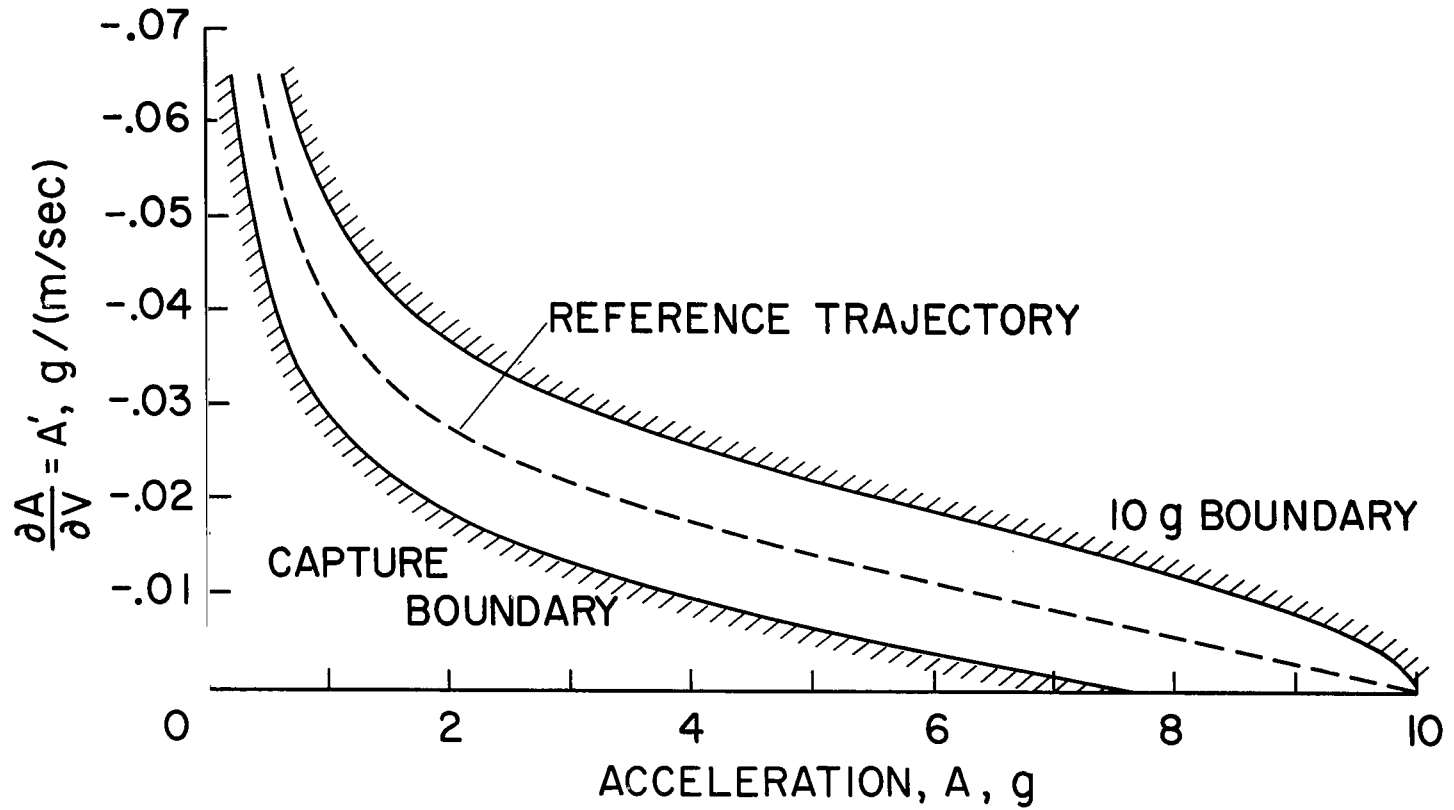
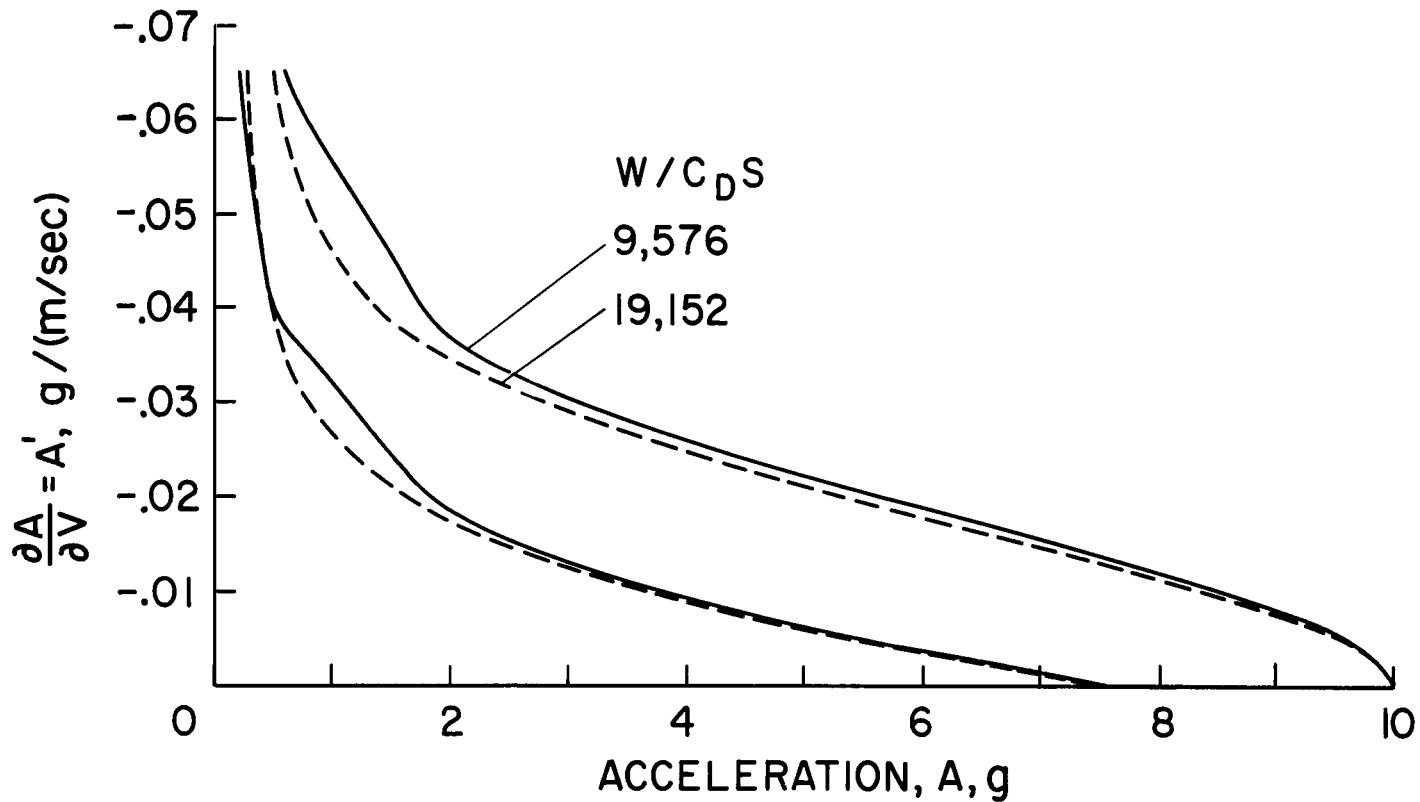
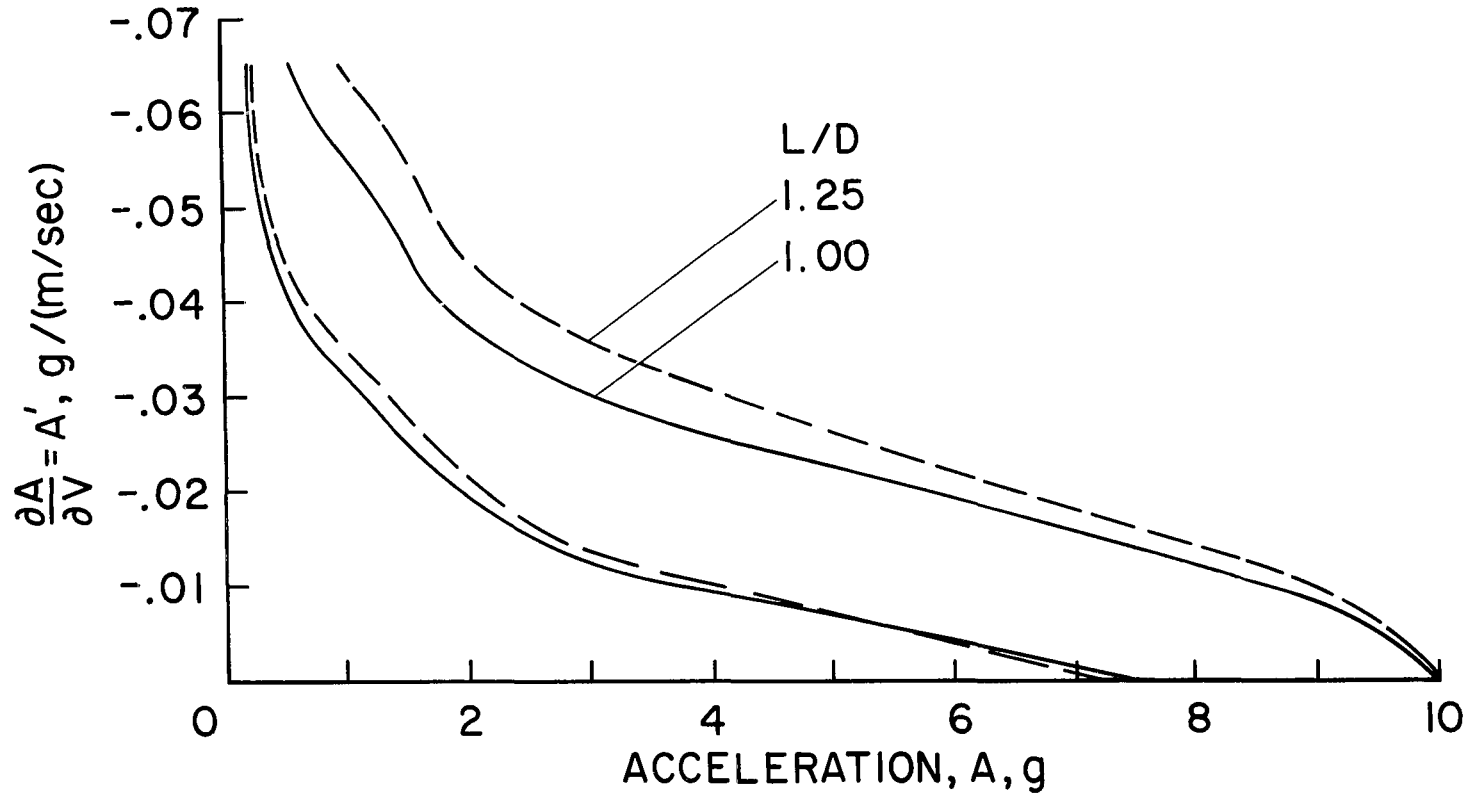


Figure 6.- Reentry boundaries and reference trajectory;  $V_i = 21,336$  m/sec,  $L/D = 1.0$ ,  
 $W/C_{DS} = 9,576$  N/m<sup>2</sup>.



(a) Ballistic parameter;  $L/D = 1.0$

Figure 7.- Effect of vehicle parameter variation on reentry boundaries;  $V_i = 21,336$  m/sec.



(b) Lift-drag ratio;  $W/C_{DS} = 9576 \text{ N/m}^2$ .

Figure 7.- Concluded.

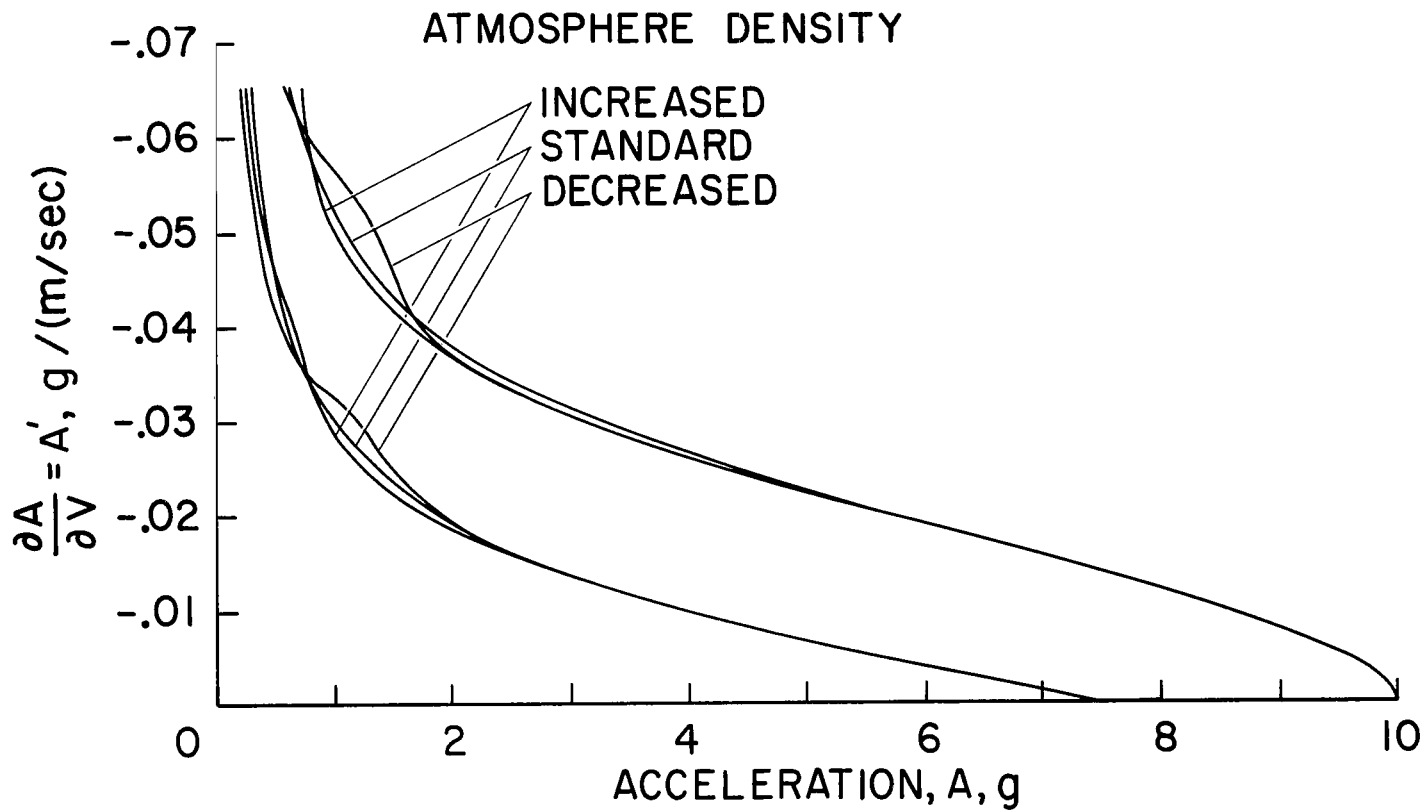


Figure 8.- Effect of atmosphere density variations on reentry boundaries;  $V_i = 21,336$  m/sec,  
 $L/D = 1.0$ ,  $W/C_D S = 9,576$  N/m<sup>2</sup>.

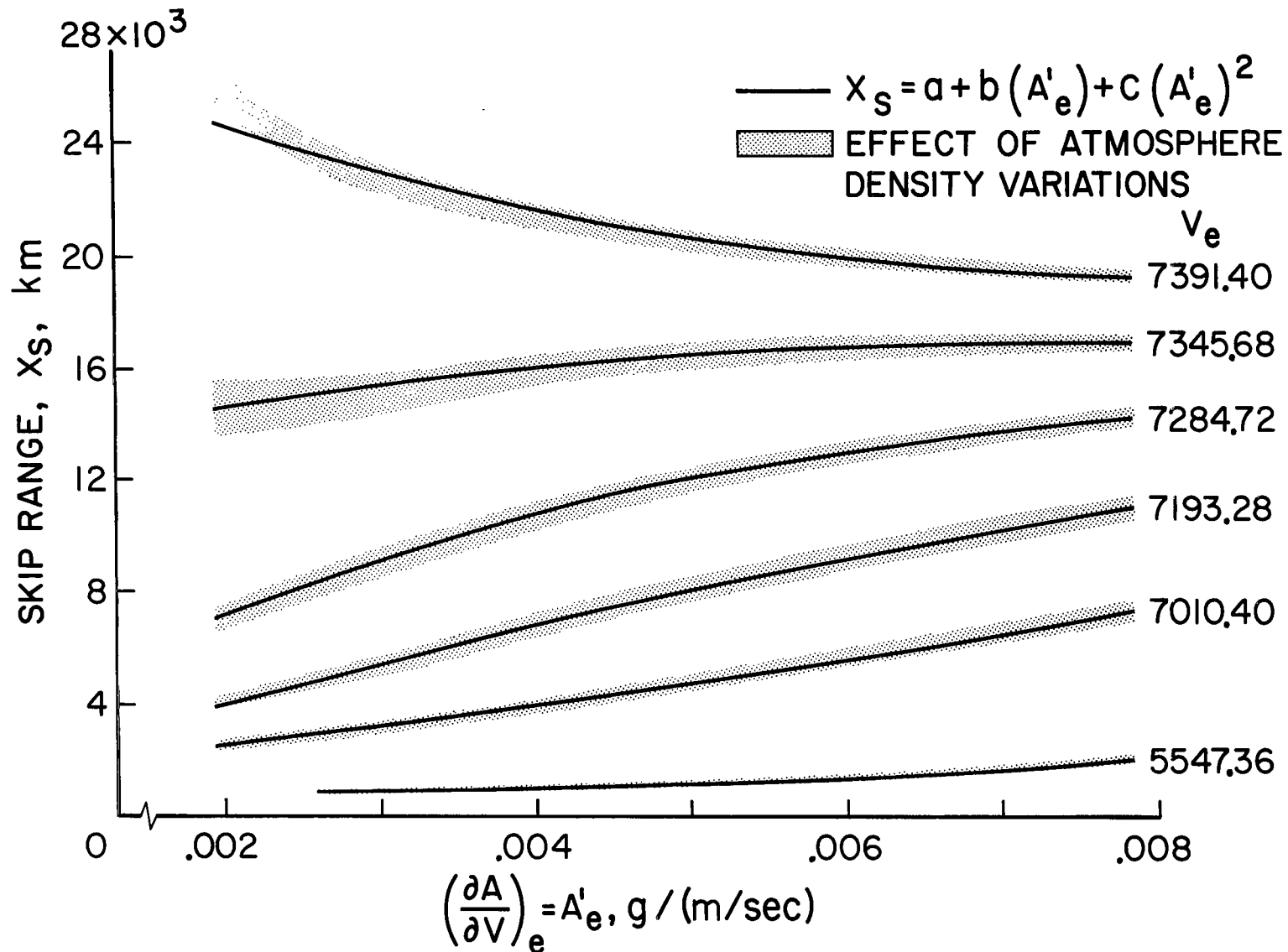


Figure 9.- Skip range as a function of atmosphere exit conditions;  $L/D = 1.0$ ,  $W/C_{DS} = 9576 \text{ N/m}^2$ .

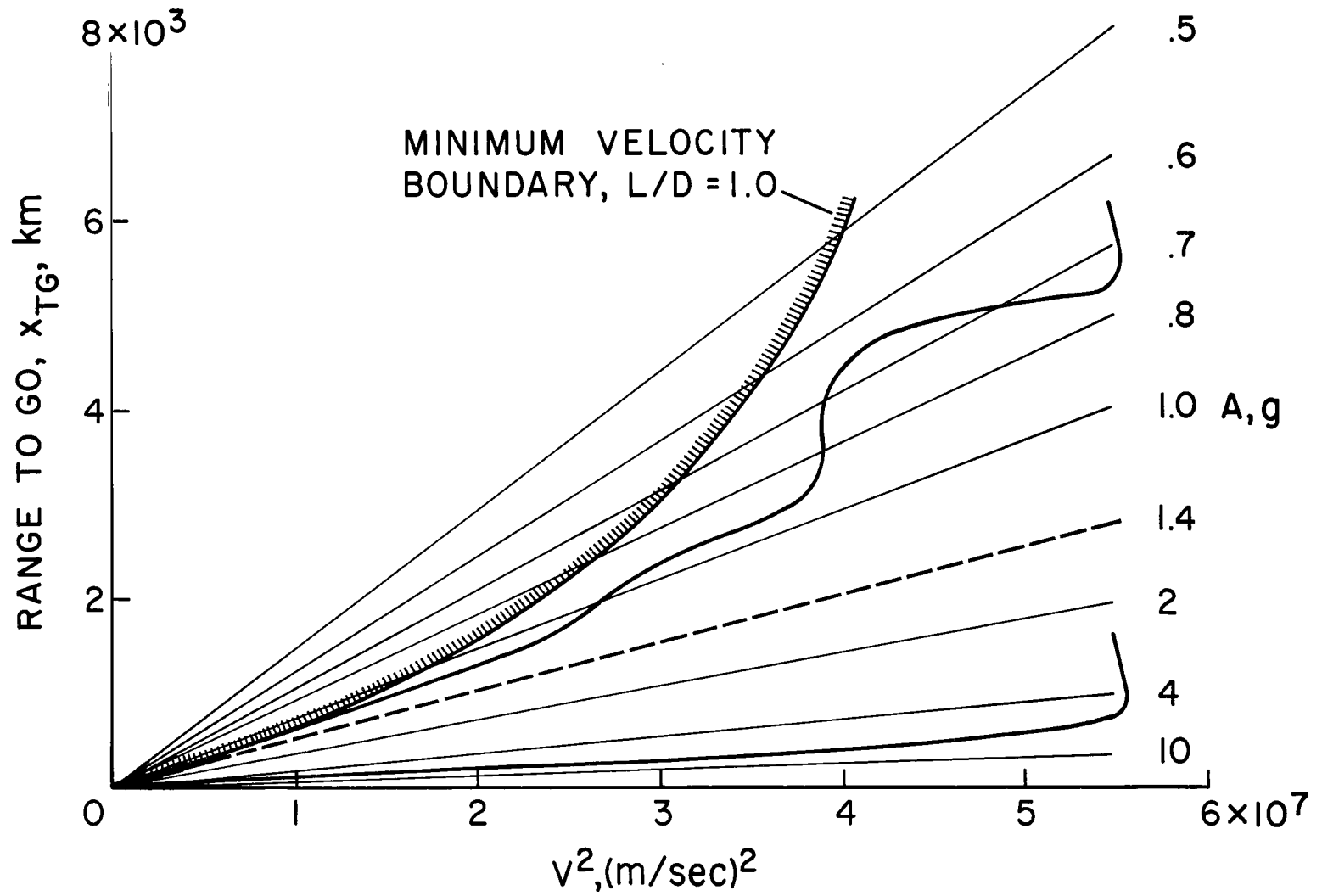


Figure 10.- Terminal control; L/D = 1.0,  $W/C_{D5} = 9576 \text{ N/m}^2$ .

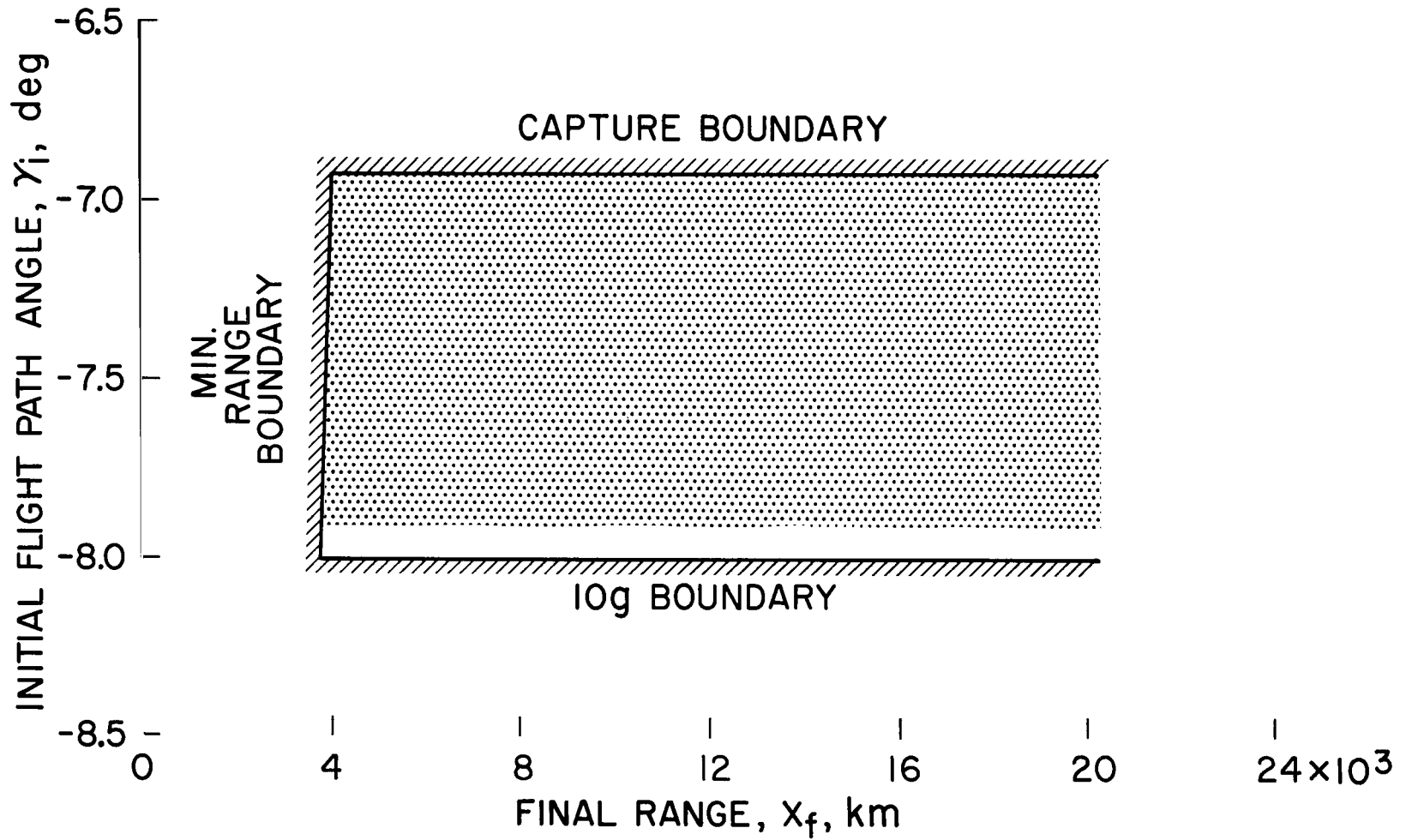


Figure 11.- Guidance capability;  $V_i = 21,336$  m/sec,  $L/D = 1.0$ ,  $W/C_{D0} = 9,576$  N/m<sup>2</sup>; standard density.

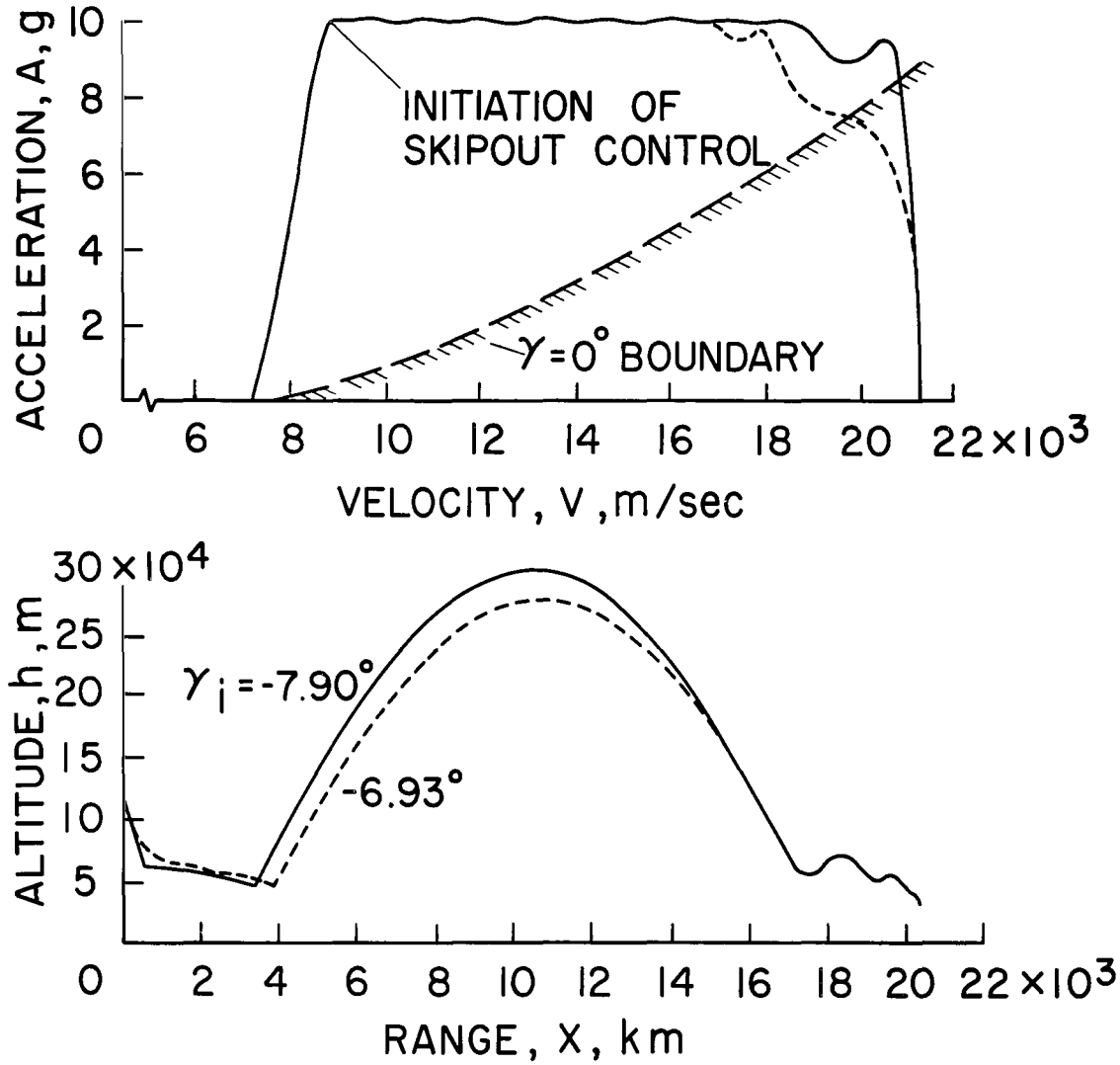


Figure 12.- Typical guided trajectories;  $L/D = 1.0$ ,  $W/C_D S = 9576 \text{ N/m}^2$ .

*"The aeronautical and space activities of the United States shall be conducted so as to contribute . . . to the expansion of human knowledge of phenomena in the atmosphere and space. The Administration shall provide for the widest practicable and appropriate dissemination of information concerning its activities and the results thereof."*

—NATIONAL AERONAUTICS AND SPACE ACT OF 1958

## NASA SCIENTIFIC AND TECHNICAL PUBLICATIONS

**TECHNICAL REPORTS:** Scientific and technical information considered important, complete, and a lasting contribution to existing knowledge.

**TECHNICAL NOTES:** Information less broad in scope but nevertheless of importance as a contribution to existing knowledge.

**TECHNICAL MEMORANDUMS:** Information receiving limited distribution because of preliminary data, security classification, or other reasons.

**CONTRACTOR REPORTS:** Technical information generated in connection with a NASA contract or grant and released under NASA auspices.

**TECHNICAL TRANSLATIONS:** Information published in a foreign language considered to merit NASA distribution in English.

**TECHNICAL REPRINTS:** Information derived from NASA activities and initially published in the form of journal articles.

**SPECIAL PUBLICATIONS:** Information derived from or of value to NASA activities but not necessarily reporting the results of individual NASA-programmed scientific efforts. Publications include conference proceedings, monographs, data compilations, handbooks, sourcebooks, and special bibliographies.

*Details on the availability of these publications may be obtained from:*

SCIENTIFIC AND TECHNICAL INFORMATION DIVISION  
NATIONAL AERONAUTICS AND SPACE ADMINISTRATION  
Washington, D.C. 20546